A new car-following model considering velocity anticipation*

Tian Jun-Fang(田钧方), Jia Bin(贾 斌)†, Li Xin-Gang(李新刚), and Gao Zi-You(高自友)

MOE Key Laboratory for Urban Transportation Complex Systems Theory and Technology, Beijing Jiaotong University, Beijing 100044, *China*

(Received 6 July 2009; revised manuscript received 17 July 2009)

The full velocity difference model proposed by Jiang *et al.* [2001 *Phys. Rev.* E **64** 017101] has been improved by introducing velocity anticipation. Velocity anticipation means the follower estimates the future velocity of the leader. The stability condition of the new model is obtained by using the linear stability theory. Theoretical results show that the stability region increases when we increase the anticipation time interval. The mKdV equation is derived to describe the kink–antikink soliton wave and obtain the coexisting stability line. The delay time of car motion and kinematic wave speed at jam density are obtained in this model. Numerical simulations exhibit that when we increase the anticipation time interval enough, the new model could avoid accidents under urgent braking cases. Also, the traffic jam could be suppressed by considering the anticipation velocity. All results demonstrate that this model is an improvement on the full velocity difference model.

Keywords: car-following, traffic flow, velocity anticipation
PACC: 0550, 0520

1. Introduction

In recent years, traffic flow theory has shown substantial development.[1−6] Many traffic models have been proposed by scientists.[7−23] Among these models, car-following models,[7−19] describing the traffic behaviour of individual vehicles, have attracted much attention for decades. In 1995, Bando *et al.*[13] presented the optimal velocity model (OVM), which is based on the idea that each vehicle has an optimal velocity, and the optimal velocity depends on the following distance from the preceding vehicle, i.e.

$$\frac{\mathrm{d}v_n}{\mathrm{d}t}(t) = \frac{1}{\tau}[V(\Delta x_n(t)) - v_n(t)], \tag{1}$$

where τ is the delay time, $1/\tau$ is the sensitivity and $V(\Delta x_n(t))$ is the optimal velocity; $\Delta x_n(t) = x_{n+1}(t) - x_n(t)$ is the space headway, $x_n(t)$ is the position of car n at time t, and $v_n(t)$ is the velocity of car n at time t. The OVM could reproduce many properties of real traffic flows, such as the instability of traffic flow, the evolution of traffic congestion, and the formation of stop-and-go waves, so it has attracted much attention.

In 1998, Helbing and Tilch[14] carried out a calibration of the OVM with respect to the empirical data. They take the optimal velocity function as follows:

$$V(\Delta x_n(t)) = v_1 + v_2 \tanh[c_1(\Delta x_n(t) - l_c) - c_2], \tag{2}$$

where l_c is the length of the vehicles, which can be taken as 5 m in simulations. The resulting optimal parameter values are $1/\tau = 0.85$, $v_1 = 6.75$ m/s, $v_2 = 7.91$ m/s, $c_1 = 0.13$, $c_2 = 1.57$. Their simulation results show that the OVM exhibits too high an acceleration and an unrealistic deceleration compared with the empirical data. Therefore, they proposed the generalized force model (GFM), i.e.

$$\frac{\mathrm{d}v_n}{\mathrm{d}t}(t) = \frac{1}{\tau}[V(\Delta x_n(t)) - v_n(t)] + \frac{\lambda}{\tau}\Theta(-\Delta v_n(t))\Delta v_n(t), \tag{3}$$

where Θ is the Heaviside function, λ is the responsive factor of velocity difference; $\Delta v_n(t)$ is the velocity difference between cars n and $n+1$, and $\tau = 2.45$ s in GFM. But Jiang *et al.*[15] found that the GFM is poor in anticipating the delay time of car motion and kinematic wave speed, so they improved the GFM and proposed the full velocity difference model (FVDM), i.e.

*Project supported by the National Basic Research Program of China (Grant No. 2006CB705500), the National Natural Science Foundation of China (Grant Nos. 70501004, 70701004 and 70631001) and the Program for New Century Talents in University, Ministry of Education, China (Grant No. NCET-07-0057).
†Corresponding author. E-mail: jiabin@jtys.bjtu.edu.cn
© 2010 Chinese Physical Society and IOP Publishing Ltd

$$\frac{\mathrm{d}v_n}{\mathrm{d}t}(t) = \frac{1}{\tau}[V(\Delta x_n(t)) - v_n(t)] + \frac{\lambda}{\tau}\Delta v_n(t). \quad (4)$$

In this paper, we improve the FVDM by considering velocity anticipation. Velocity anticipation means the follower estimates the future velocity of the leader. Although this effect has already been considered in many cellular automata models,[24−26] until now few car-following models have considered this effect.[27,28] In the following section, the improved model will be introduced. In Section 3, linear stability analysis is applied to obtain the neutral line. In Section 4, the mKdV equation is derived by nonlinear stability analysis to describe the kink–antikink soliton wave and obtain the coexisting stability line. In Section 5, simulations are carried out. Finally, the conclusions are given in Section 6.

2. The new model

In real traffic, drivers always anticipate the velocity of their leading cars in the next moment. They always judge the variation tendency of the velocity of their leading cars, i.e., whether the leading cars will accelerate, decelerate or just keep a steady velocity. According to these, they could adjust their speed in time. Furthermore, these are very important to avoid crashing, especially in some urgent braking cases, such as at traffic lights or car accidents. When an accident occurs in front of the leader, the follower can also see the accident at almost the same time as his leader. Therefore, he knows that his leader will decelerate, so his reaction to the accident is almost at the same time with his leader. In a word, the follower will adjust his speed by considering the anticipation velocity of the leader in the next moment according to the driving conditions. As we know, anticipation velocity has already been considered in many cellular automata models, but until now few car-following models have considered this effect. In this paper, this effect will be taken into account on the basis of FVDM. The anticipation velocity of the leader is given in the form of $v_{n+1}(t+\alpha\tau)$, representing that the follower could anticipate the leader's velocity in the next moment $t+\alpha\tau$. α is a coefficient, and the anticipation time interval $\alpha\tau$ should not be too large. Since human drivers' estimation ability is limited, the larger the $\alpha\tau$ is, the greater the error caused by anticipation is. We will give the variation range of $\alpha\tau$ in the next section. Replacing $v_{n+1}(t)$ by $v_{n+1}(t+\alpha\tau)$ in FVDM, we could obtain

$$\begin{aligned}\frac{\mathrm{d}v_n}{\mathrm{d}t}(t) &= \frac{1}{\tau}[V(\Delta x_n(t)) - v_n(t)] \\ &\quad + \frac{\lambda}{\tau}[v_{n+1}(t+\alpha\tau) - v_n(t)], \end{aligned} \quad (5)$$

where we calculate $v_{n+1}(t+\alpha\tau)$ by $v_{n+1}(t+\alpha\tau) = v_{n+1}(t) + \alpha\tau a_{n+1}(t)$ for simplicity; and $a_{n+1}(t)$ is the acceleration of the leader. So, we could obtain

$$\begin{aligned}\frac{\mathrm{d}v_n}{\mathrm{d}t}(t) &= \frac{1}{\tau}[V(\Delta x_n(t)) - v_n(t)] \\ &\quad + \frac{\lambda}{\tau}[v_{n+1}(t) - v_n(t)] + \frac{\lambda}{\tau}\alpha\tau a_{n+1}(t). \end{aligned} \quad (6)$$

Then, the new model is given as follows:

$$\begin{aligned}\frac{\mathrm{d}v_n}{\mathrm{d}t}(t) &= \frac{1}{\tau}[V(\Delta x_n(t)) - v_n(t)] \\ &\quad + \frac{\lambda}{\tau}\Delta v_n(t) + \lambda\alpha a_{n+1}(t). \end{aligned} \quad (7)$$

We call $\lambda\alpha a_{n+1}(t)$ the anticipation term. One can see that the difference between the new model and FVDM is that the FVDM does not have the anticipation term.

3. Linear stability analysis

Linear stability analysis can be conducted for the new model. It is obvious that the steady state is that vehicles move with uniform space headway Δx_0, and the optimal velocity function $V = V(\Delta x_0)$. So, the steady-state solution is given by

$$x_n^{(0)}(t) = \Delta x_0 n + Vt, \quad \Delta x_0 = L/N, \quad (8)$$

where N is the number of cars, L is the road length. For convenience, we use $\kappa, \lambda_1, \lambda_2$ to represent $1/\tau$, λ/τ, $\lambda\alpha$ respectively, thus κ is the sensitivity. Suppose that $y_n(t)$ is a small deviation from the steady-state solution: $x_n(t) = x_n^{(0)}(t) + y_n(t)$. Then, the linear equation is obtained from Eq. (7),

$$\begin{aligned}\frac{\mathrm{d}^2 y_n(t)}{\mathrm{d}t^2} &= \kappa\left[V'\Delta y_n(t) - \frac{\mathrm{d}y_n(t)}{\mathrm{d}t}\right] \\ &\quad + \lambda_1\frac{\mathrm{d}\Delta y_n(t)}{\mathrm{d}t} + \lambda_2\frac{\mathrm{d}^2 y_{n+1}(t)}{\mathrm{d}t^2}, \end{aligned} \quad (9)$$

where

$$V' = \frac{\mathrm{d}V(\Delta x)}{\mathrm{d}\Delta x}|_{\Delta x=\Delta x_0}.$$

By expanding $y_n(t) = \exp(\mathrm{i}\,\alpha_k n + zt)$, the following equation of z is obtained

$$\begin{aligned}z^2(1 - \lambda_2\exp(\mathrm{i}\,\alpha_k)) &= \kappa(V'(\exp(\mathrm{i}\,\alpha_k) - 1) - z) \\ &\quad + \lambda_1 z(\exp(\mathrm{i}\,\alpha_k) - 1), \end{aligned} \quad (10)$$

in which $z = vi$ is taken, v is a real number. Setting its real part and imaginary part to be equal to zero, we could have

$$-v^2 = \kappa V'(\cos(\alpha_k) - 1) - \lambda_1 v \sin(\alpha_k) - \lambda_2 v^2 \cos(\alpha_k), \quad (11)$$

$$0 = \kappa V' \sin(\alpha_k) - \kappa v + \lambda_1 v \cos(\alpha_k) - \lambda_1 v - \lambda_2 v^2 \sin(\alpha_k). \quad (12)$$

From Eqs. (11) and (12), one obtains,

$$v = \frac{\kappa V' \sin(\alpha_k)(\lambda_2 - 1)}{\sigma}, \quad (13)$$

where $\sigma = (\kappa\lambda_2 + \lambda_1\lambda_2 + \lambda_1)\cos(\alpha_k) - (\kappa + \lambda_1 + \lambda_1\lambda_2)$. Substituting Eq. (13) into Eq. (10), one has

$$V' = \frac{\sigma(\kappa\lambda_2 \cos(\alpha_k) + 2\lambda_1\lambda_2)(\cos(\alpha_k) - 1)}{\kappa \sin^2(\alpha_k)(\lambda_2 - 1)^2\lambda_2}; \quad (14)$$

when $\alpha_k \to 0$, we obtain the stable condition

$$V' < \frac{\kappa/2 + \lambda_1}{1 - \lambda_2}. \quad (15)$$

Taking each parameter to the original one, we could have

$$V' < \frac{1 + 2\lambda}{2\tau(1 - \alpha\lambda)}. \quad (16)$$

One can see that

$$\alpha\lambda < 1, \quad \alpha\tau < \frac{\tau}{\lambda}, \quad (17)$$

i.e., the anticipation time interval $\alpha\tau$ should not be larger than τ/λ. If $\alpha = 0$, we could obtain the stable condition of the FVDM

$$V' < \frac{1 + 2\lambda}{2\tau}. \quad (18)$$

Figure 1 shows the neutral stability curves of FVDM and the new model in the phase space. One can see that the unstable region of the new model is smaller than that of FVDM, i.e., the stability condition can be satisfied more easily than previous models. From Fig. 1, one can see that with increasing α, the critical sensitivity κ_c decreases, and the case of $\alpha = 0$ corresponds to the FVDM model. It means that traffic will become stable, with the increase of α. This phenomenon is in accordance with real traffic. However, as we have said, the anticipation time interval $\alpha\tau$ should not be too large, because up to now, vehicles on the highway are mostly manually manipulated. A larger anticipation time interval will lead to a larger error due to the limitations of human drivers' estimation ability. But with the increasingly widespread application of the intelligent transportation system, it is possible to use a larger $\alpha\tau$.

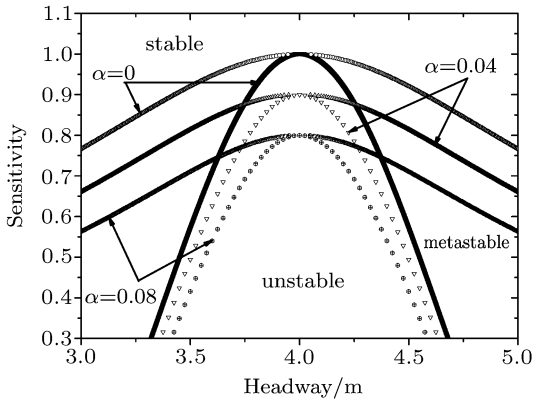


Fig. 1. Phase diagram for the headway–sensitivity space. The neutral stability curves are given based on Eq. (15). The space is divided into three regions by the neutral stability curve and the coexisting stability curve: stable region, metastable region and unstable region.($V_{\max} = 2$, $h_c = 4$, $\tau = 2.45$, $\lambda = 1.225$).

4. Nonlinear stability analysis

For later convenience, Eq. (7) is rewritten in the different form

$$\frac{\mathrm{d}^2\Delta x_n(t)}{\mathrm{d}t^2} = \kappa\Big[V(\Delta x_{n+1}(t)) - V(\Delta x_n(t)) - \frac{\mathrm{d}\Delta x_n(t)}{\mathrm{d}t}\Big] + \lambda_1\Big(\frac{\mathrm{d}\Delta x_{n+1}(t)}{\mathrm{d}t} - \frac{\mathrm{d}\Delta x_n(t)}{\mathrm{d}t}\Big) + \lambda_2\frac{\mathrm{d}^2\Delta x_{n+1}(t)}{\mathrm{d}t^2}. \quad (19)$$

We choose the form of function $V(\Delta x_{n+1}(t))$ proposed by Bando *et al.*[13] for the convenience of nonlinear analysis, i.e.

$$V(\Delta x_n(t)) = \frac{V_{\max}}{2}[\tanh(\Delta x_n(t) - h_c) + \tanh(h_c)], \quad (20)$$

where h_c is the safety distance and $V_{\max}$ is the maximum velocity (for simplicity, $V_{\max} = 2$). The mKdV equation is derived just below the critical point. We use the slow variables X and T defined as follows:[29]

$$X = \varepsilon(n + bt), \qquad T = \varepsilon^3 t, \quad (21)$$

where b is a constant to be determined later. The headway is set as

$$\Delta x_n(t) = h_c + \varepsilon R(X, T). \quad (22)$$

By expanding each term in Eq. (19) to the fifth order of ε with the use of Eqs. (21) and (22), we have the following equation

$$\varepsilon^2(b-V')\kappa\partial_X R \quad +\varepsilon^3\left[b^2-\kappa\frac{V'}{2}-\lambda_1 b-\lambda_2 b\right]\partial_X^2 R+\varepsilon^4\left[\kappa\partial_T R-\left(\lambda_2 b^2+\frac{\lambda_1 b}{2}+\frac{\kappa V'}{6}\right)\partial_X^3 R-\frac{\kappa V'''}{6}\partial_X R^3\right]$$
$$+\varepsilon^5\left[(2b-\lambda_1-2\lambda_2 b)\partial_X\partial_T R-\left(\frac{\kappa V'}{24}+\frac{b}{6}-\frac{\lambda_2 b^2}{2}\right)\partial_X^4 R-\frac{\kappa V'''}{12}\partial_X^2 R^3\right]=0, \tag{23}$$

where

$$V'=\frac{\mathrm{d}V(\Delta x)}{\mathrm{d}\Delta x}|_{\Delta x=h_c}, \quad V'''=\frac{\mathrm{d}^3V(\Delta x)}{\mathrm{d}\Delta x^3}|_{\Delta x=h_c}.$$

Around the critical point we have $(\kappa_c/\kappa)-1=\varepsilon^2$, $V'=((\kappa_c/2)+\lambda_1)/(1-\lambda_2)$; by taking $b=V'$, Eq. (23) becomes

$$\varepsilon^4[\partial_T R-g_1\partial_X^3 R+g_2\partial_X R^3]+\varepsilon^5[g_3\partial_X^2 R+g_4\partial_X^4 R+g_5\partial_X^2 R^3]=0, \tag{24}$$

where

$$g_1=\frac{V'}{6}+\frac{\lambda_1 V'}{2\kappa}+\frac{\lambda_2 V'^2}{\kappa}, \quad g_2=-\frac{V'''}{6}, \quad g_3=\frac{V'}{2},$$
$$g_4=\frac{2V'-\lambda_1}{\kappa}\left(\frac{V'}{6}+\frac{\lambda_1 V'}{2\kappa}+\frac{\lambda_2 V'^2}{\kappa}\right)-\frac{V'}{24}-\frac{V'\lambda_1}{6\kappa}+\frac{2\lambda_2 V'}{\kappa}, \quad g_5=\frac{2V'V'''-\lambda_1 V'''}{6\kappa}-\frac{V'''}{12}.$$

In order to derive the standard mKdV equation, we make the following transformations:

$$T'=g_1 T, \quad R=\sqrt{\frac{g_1}{g_2}}R'.$$

So, equation (24) turns into

$$\partial_{T'}R'-\partial_X^3 R'+\partial_X R'^3+\varepsilon M[R']=0, \tag{25}$$

where

$$M[R']=\sqrt{\frac{1}{g_1}}\left(g_3\partial_X^2 R'+\frac{g_1 g_5}{g_2}\partial_X^2 R'^3+g_4\partial_X^4 R'\right).$$

Equation (25) is the mKdV equation with $O(\varepsilon)$ being a correction term. We ignore the $O(\varepsilon)$ term and obtain the mKdV equation with the kink–antikink soliton solution

$$R_0'(X,T')=\sqrt{c}\tanh\left[\sqrt{\frac{c}{2}}(X-cT')\right]. \tag{26}$$

Suppose $R'(X,T')=R_0'(X,T')+\varepsilon R_1'(X,T')$. In order to determine the value of the propagation velocity for the kink–antikink soliton solution, it is necessary to satisfy the following condition

$$(R_0', M[R_0'])\equiv\int_{-\infty}^{+\infty}\mathrm{d}X R_0' M[R_0']=0, \tag{27}$$

where $M[R_0']=M[R']$. By solving this equation, we obtain the selected value c[30]

$$c=\frac{5g_2g_3}{2g_2g_4-3g_1g_5}. \tag{28}$$

Hence, we obtain the kink–antikink soliton solution($V'=V_{\max}/2=1, V'''=-V_{\max}=-2$),

$$\Delta x_n(t)=\Delta x_0+\sqrt{\frac{g_1 c}{g_2}\left|1-\frac{\kappa_c}{\kappa}\right|}\tanh\left\{\sqrt{\frac{c}{2}\left|1-\frac{\kappa_c}{\kappa}\right|}\times\left[n+\left(1-cg_1\left|1-\frac{\kappa_c}{\kappa}\right|\right)t\right]\right\}. \tag{29}$$

The amplitude A of the solution is

$$A=\sqrt{\frac{g_1}{g_2}\left(\frac{\kappa_c}{\kappa}-1\right)c}, \tag{30}$$

where $\kappa_c=2V'(1-\lambda_2)-2\lambda_1$. Rewriting each variable to the original one, we obtain

$$c=\frac{60(1-\lambda_1-\lambda_2)^2}{12+3\lambda_1-53\lambda_1\lambda_2+86\lambda_2-38\lambda_2^2}, \tag{31}$$

$$A=\sqrt{\frac{(\kappa+3\lambda_1+6\lambda_2)(2-2\lambda_1-2\lambda_2-\kappa)}{2\kappa^2}c}. \tag{32}$$

The kink–antikink solution represents the coexisting phase, which includes both the freely moving phase and the jam phase. The headway of the freely moving phase is given by $\Delta x=h_c+A$. The headway of the jam phase is given to be $\Delta x=h_c-A$.[31] Then, we obtain the coexisting curve in the headway–sensitivity space. Figure 1 shows the coexisting curves and the neutral stability curves. For each pair of curves, the space is divided into three regions, i.e. the stable region, the metastable region and the unstable region.

5. Simulation

In the following simulation, the parameters of the new model are listed in Table 1. We choose Eq. (2) as the optimal function. It can be seen that when $\alpha = 0.04$, we obtain $\lambda\alpha \approx 0.05$ and the anticipation time interval $\alpha\tau \approx 0.1$ s. When $\alpha = 0.08$, we have $\lambda\alpha \approx 0.1$ and $\alpha\tau \approx 0.2$ s. Both values meet Eq. (17). So, the anticipation time interval is very small during the following simulation.

Table 1. Values of δt and C_j in FVDM and COVM.

model	δt/s	C_j/(km/h)
FVDM ($\tau = 2.45$ s, $\lambda = 1.225$, $\alpha = 0$)	1.4	19.03
new model ($\tau = 2.45$ s, $\lambda = 1.225$, $\alpha = 0.04$)	1.37	19.40
new model ($\tau = 2.45$ s, $\lambda = 1.225$, $\alpha = 0.08$)	1.33	20.02

Firstly, we simulate the vehicles' behaviours under the urgent braking case based on Ref. [16]. The urgent braking case can be as follows: a freely moving car decelerates drastically for an accident in front of it or a red light at an intersection, and the following car is freely moving while the distance between the two cars is quite small. In this paper, the simulation under such a situation is carried out as the following. Two successive cars move with the same speed 14.5 m/s at the initial time $t = 0$ and the space headway is 20 m. The leading car decelerates suddenly with the deceleration -8 m/s^2 until it stops completely. The leading car remains standing for several seconds before accelerating back to its original speed. The simulation results are shown in Fig. 2(a), which exhibits the variation of space headway of the following car. We can see that the space headways are smaller than 5 m when $\alpha = 0$ (FVDM) and $\alpha = 0.04$; this indicates that the leader and the follower collide. When $\alpha = 0.08$, the space headway is always larger than 5 m, i.e., the accident has been successfully avoided. Secondly, the delay time of car motion δt and kinematic wave speed C_j at jam density are examined in the new model. We carried out the same simulation as that in Ref. [15]. First a traffic signal is yellow and all vehicles are waiting with headway 7.4 m, at which the optimal velocity is zero. Then at time $t = 0$, the signal changes to green and cars begin to move. The simulation results are shown in Figs. 3(a), 3(b), 3(c) and Table 1. From Table 1, we can see that when $\alpha = 0.04$, the values of δt and C_j are 1.37 s and 19.40 m/s, and when $\alpha = 0.08$, the values of δt and C_j are 1.33 s and 20.02 m/s. As Bando *et al.* pointed out, the observed δt is of the order of 1 s,[32] and Del Castillo and Benitez indicated that C_j ranges between 17 and 23 km/h.[33] So, the new model is successful in anticipating the two parameters.

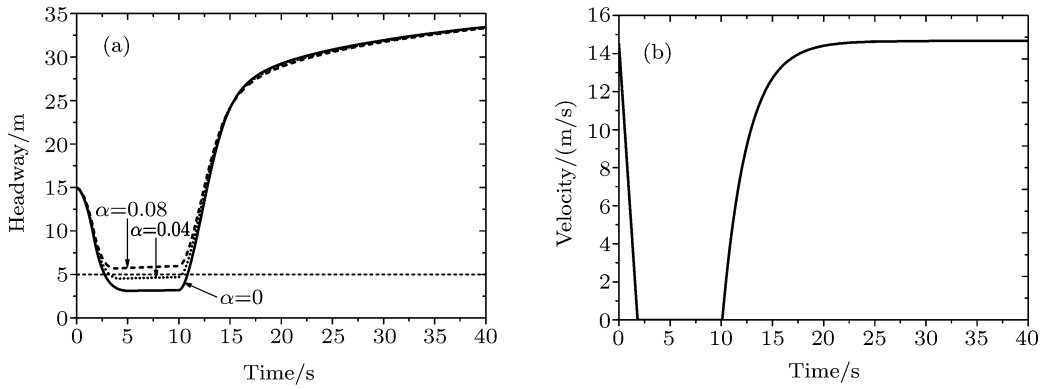


Fig. 2. Simulations for different values of α under an urgent case. (a) The headway distance of the follower. (b) The velocity of the leader.

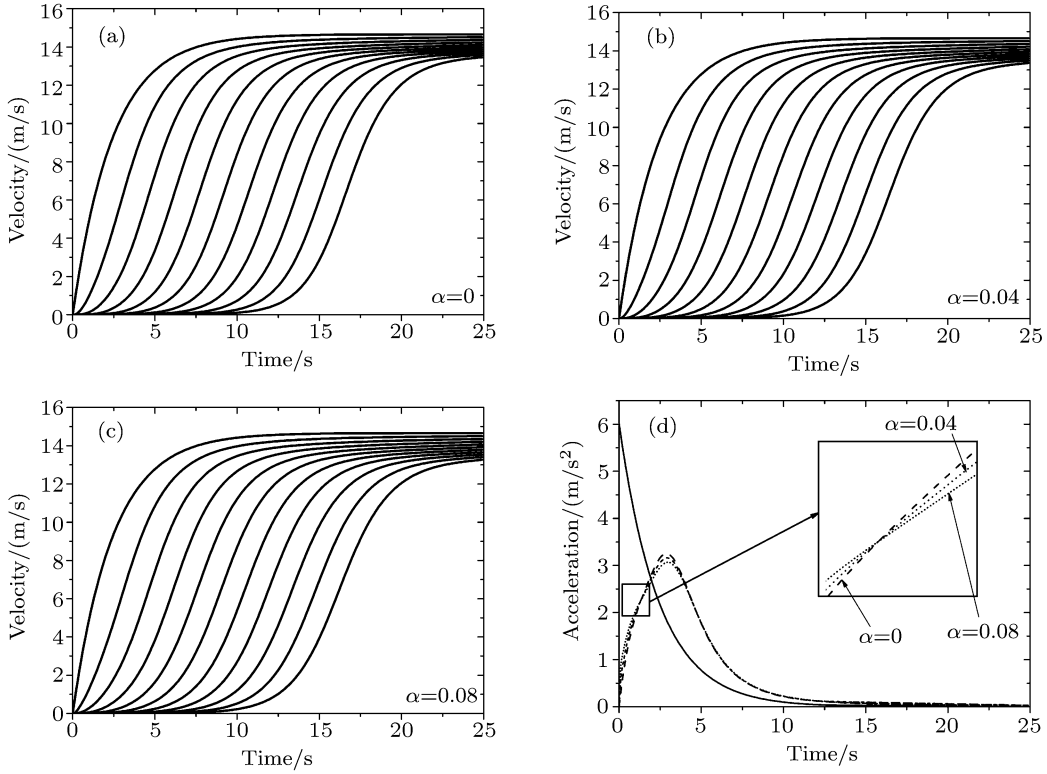


Fig. 3. The velocity of all vehicles starting from a traffic signal for different values of α: (a) $\alpha = 0$, (b) $\alpha = 0.04$ and (c) $\alpha = 0.08$. (d) The accelerations of an unobstructed leading car and its following car; both initially are at rest for different α.

Figure 3(d) shows the variation of acceleration in the case that two successive cars are initially at rest, and the leading car is unobstructed. At $t = 0$, they begin to start up. We can see that the maximum value of the leading car's acceleration is the same for different α. As for the following car, the car accelerates more quickly for a larger α at the initial stage, so the delay time decreases with the increase of α. Next, a numerical simulation is carried out to investigate the traffic behaviour in the new model, similar to Ref. [15]. There are $N = 100$ vehicles running on a circular road whose length is $L = 1500$ m. The initial disturbance is set as below:

$$x_1(0) = 1 \text{ m}, \quad x_n(0) = (n-1)L/N \text{ m}, \quad n \neq 1; \tag{33}$$

$$v_n(0) = V(L/N). \tag{34}$$

The velocities of all vehicles at $t = 300$ and 2000 s are shown in Figs. 4(a) and 4(b). We can see that the traffic

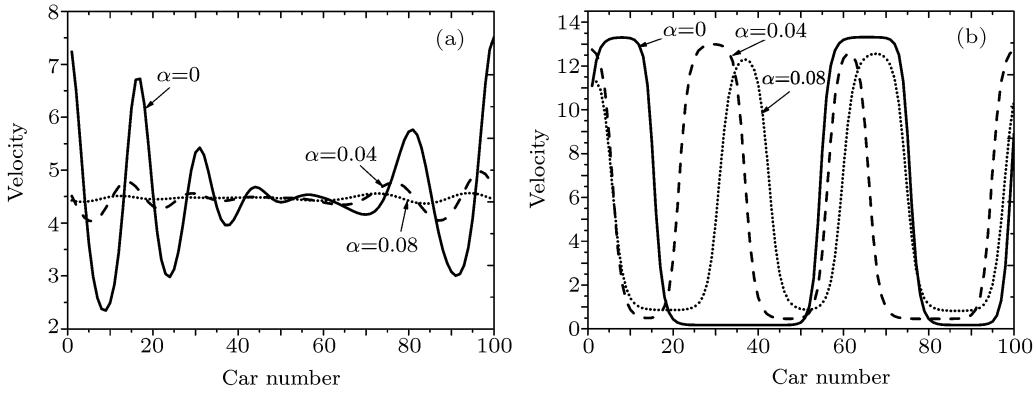


Fig. 4. The velocity of all vehicles for different values of α. (a) $t = 300$ s; (b) $t = 2000$s.

flow transforms from free flow at the initial stage to congested flow with evolution of the time for different values of α. With the increase of α, the amplitude of fluctuations reduces. Furthermore, it can be seen that with the increase of α, the velocity in congested traffic increases. When $\alpha = 0$ (FVDM), the velocity in congested traffic is almost zero, but when $\alpha = 0.08$, the velocity in congested traffic is almost 0.85 m/s. Thus, we could conclude that by considering the anticipation velocity of the leader, the follower could make a rapid reaction to the variation of the velocity of the leader. As a result, the traffic jam could be suppressed. Figure 5 shows hysteresis loops for different α. It can be seen that when α becomes bigger, the loops become smaller in size.

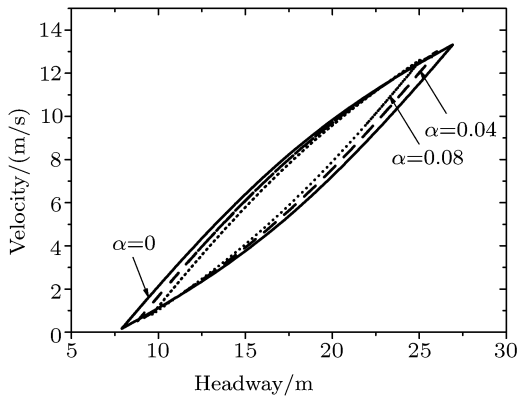


Fig. 5. Hysteresis loops for different α.

6. Conclusions

We have improved the FVDM by considering velocity anticipation. The neutral stability line is obtained by using the linear stability theory. Moveover, we derived the mKdV equation to describe the kink–antikink soliton wave and obtained the coexisting stability line. In the phase diagram for headway–sensitivity space, the neutral stability lines and coexisting stability lines are given for different values of α. We can see that with the increase of α, the stability region in the phase diagram increases. Numerical simulations were carried out for different circumstances. Results show that when the value of α is big enough, the new model could avoid accidents in the urgent braking case. The delay time of car motion δt and kinematic wave speed C_j at jam density are obtained using the new model, and are consistent with the experimental data. The phase transition from free flow to congested flow is observed, and traffic jams become more serious when we decrease the value of α. All results show that this model is an improvement of the FVDM.

References

[1] Chowdhury D, Santen L and Schadschneider A 2000 *Phys. Rep.* **329** 199
[2] Helbing D 2001 *Rev. Mod. Phys.* **73** 1067
[3] Kerner B S 2004 *The Physics of Traffic* (Heidelberg: Springer)
[4] Nagatani T 2002 *Rep. Prog. Phys.* **65** 1331
[5] Helbing D 2000 *Traffic and Granular Flow'99* (Heidelberg: Springer)
[6] Jia B, Gao Z Y, Li K P and Li X G 2007 *Models and Simulations of Traffic System Based on the Theory of Cellular Automaton* (Beijing: Science) (in Chinese)
[7] Reuschel A 1950 *Oesterreichisches Ingenieur-Archiv* **4** 193
[8] Pipes L A 1953 *J. Appl. Phys.* **24** 274
[9] Chandler R E, Herman R and Montrol E W 1958 *Oper. Res.* **6** 165
[10] Herman R and Potts R B 1961 *Proceedings-Symposium on Theory of Traffic Flow* (New York: Elsevier)
[11] Herman R, Montrol E W, Potts R B and Rothery R W 1959 *Oper. Res.* **7** 86
[12] Newell G F 1961 *Oper. Res.* **9** 209
[13] Bando M, Hasebe K, Nakayama A, Shibata A and Sugiyama Y 1995 *Phys. Rev.* E **51** 1035
[14] Helbing D and Tilch B 1998 *Phys. Rev.* E **58** 133
[15] Jiang R, Wu Q S and Zhu Z J 2001 *Phys. Rev.* E **64** 017101
[16] Zhao X M and Gao Z Y 2005 *Eur. Phys. J.* B **47** 145
[17] Treiber M, Hennecke A and Helbing D 2000 *Phys. Rev.* E **62** 1805
[18] Tang T Q, Huang H J, Wong S C and Jiang R 2009 *Chin. Phys.* B **18** 0975
[19] Xie D F, Gao Z Y and Zhao X M 2008 *Chin. Phys.* B **17** 4440
[20] Hu S X, Gao K, Wang B H and Lu Y F 2008 *Chin. Phys.* B **17** 1863
[21] Jiang R, Jin W L and Wu Q S 2008 *Chin. Phys.* B **17** 829
[22] Gao K, Wang B H, Fu C J and Lu Y F 2007 *Chin. Phys.* **16** 3483
[23] Tang C F, Jiang R and Wu Q S 2007 *Chin. Phys.* **16** 1570
[24] Li X B, Wu Q S and Jiang R 2001 *Phys. Rev.* E **64** 066128
[25] Knospe W, Santen L, Schadschneider A and Schreckenberg M 2000 *J. Phys.* A **33** L477
[26] Jiang R and Wu Q S 2003 *J. Phys.* A: *Math. Gen.* **36** 381
[27] Eissfeldt N and Wagner P 2003 *Eur. Phys. J.* B **33** 121
[28] Treiber M, Kesting A and Helbing D 2006 *Physica* A **360** 71
[29] Muramatsu M and Nagatani T 1999 *Phys. Rev.* E **60** 180
[30] Ge H X, Cheng R J and Dai S Q 2005 *Physica* A **357** 466
[31] Nagatani T 1999 *Phys. Rev.* E **60** 6395
[32] Bando M, Hasebe K, Nakanishi K and Nakayama A 1998 *Phys. Rev.* E **58** 5429
[33] Del Castillo J M and Benitez F G 1995 *Transp. Res. Part B: Methodol.* **29** 373